

BEHAVIOR OF HEADED STUD SHEAR CONNECTOR UNDER CYCLIC LOADING

Md. Belal Hossain^{*1}, Md. Khasro Miah² and A. K. M. Ruhul Amin³

¹*Post Graduate Student, Department of Civil Engineering, DUET, Gazipur, Bangladesh,
e-mail: belal.ce31stduet@gmail.com*

²*Professor, Department of Civil Engineering, DUET, Gazipur, Bangladesh, e-mail: mkhasro@duet.ac.bd*

³*Doctoral Student, Department of Civil Engineering, DUET, Gazipur, Bangladesh,
e-mail: akm.ruhul69@gmail.com*

***Corresponding Author**

ABSTRACT

Headed stud shear connectors are used in steel-concrete composite systems to ensure effective shear transfer and composite action. Although the behavior of these connectors under monotonic loading is widely explored, limited research has been conducted on how they perform under cyclic loading. This study presents a detailed numerical investigation of the behavior of headed stud shear connectors subjected to both monotonic and cyclic loads using a monlinear three-dimensional finite element model in ANSYS Workbench. The model is validated against published experimental work under monotonic loading and used for the numerical analysis under monotonic and cyclic loads. Under alternating loading, the connectors exhibit reduced shear stiffness, significant slip accumulation, and increased stress concentration around the stud base, eventually leading to localized stud yielding and concrete crushing. The responses under the loading regimes demonstrated that cyclic effects can substantially influence the performance and long-term durability of the headed stud shear connectors. These findings emphasize the need to integrate alternating load behavior in the design and assessment of composite structural components, particularly those used to construct bridges and transport infrastructure.

Keywords: *Headed Stud Shear Connectors; Monotonic and Alternating Loads; Ansys Simulation; Cyclic Behavior; Finite Element Analysis (Fea).*

INTRODUCTION

Steel concrete composite buildings are becoming a prominent construction technology worldwide. Due to increased traffic demand, the number of bridges is fast increasing in both developed and developing countries. In this sense, given the high-speed traffic movement and span, composite bridges are a critical resource for addressing traffic demand. To achieve the composite action in composite bridges, proper shear stud connectors are used to connect the steel and concrete parts. The composite action created by the shear stud connection improves the strength, ductility, and durability of the structures. In our nation, the number of composite structures has been gradually rising. Studs are welded to a steel girder and implanted in the concrete to provide the composite action between steel and concrete. The head of the stud prevents separation from the concrete slab. A number of researchers looked into the behavior of shear stud connectors from different perspectives. Among these, (Viest, 1956) examined full-scale push-out specimens and discovered that steel studs work well as shear connectors in composite constructions. The diameter and concrete strength determine the shear stud connections' strength. According to Feyissa and Kenea (2022) and Lu (2023), the shear stud connector's performance increases with the increase in stud diameter and concrete strength. Stud height, embedded concrete strength, stud spacing, and failure patterns were all taken into account when assessing the shear stud connectors' capacity (Wang, 2021). The slip behavior and strain at the base and mid-height of the stud shank in composite structures were investigated in a pull-out specimen (Miah, 2010). It is found from the literature that experimental and numerical studies exist on headed stud shear connectors under monotonic loading, whereas limited numerical investigations have addressed their cyclic load behavior. To address this gap, experimental results of push and pull-out specimens (Miah, 2005) will be simulated numerically using ANSYS software. To validate that the numerical model is of research interest. After validation, the shear capacity and shear stiffness of the shear connector under monotonic and cyclic loading will be investigated through a parametric study.

2. FINITE ELEMENT MODELING

The numerical study was done with ANSYS library material properties that had been changed. The succeeding section describes various types of elements that are used for numerical simulation.

2.1 Geometry of the Experimental Specimen

The push and pull-out test specimen with the generally used solid stud was employed for the experimental investigation shown in Figure 1. Monotonic as well as cyclic loading can be applied easily to this specimen to observe the behavior of the stud shear connectors.

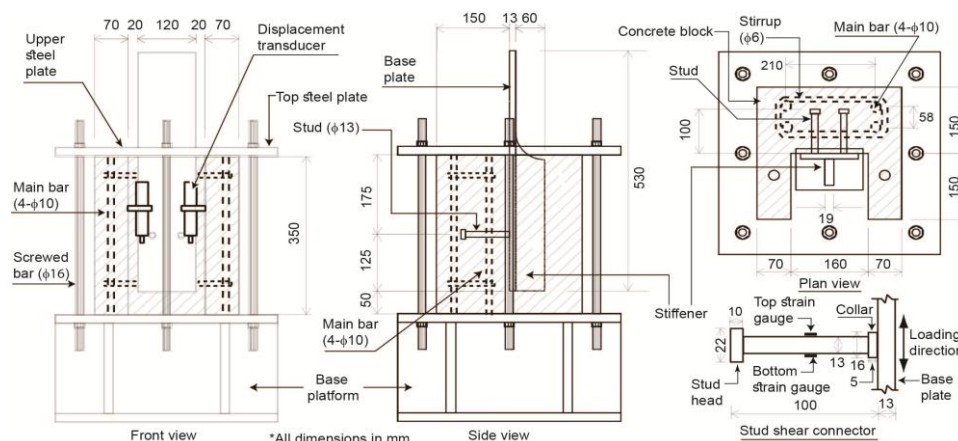
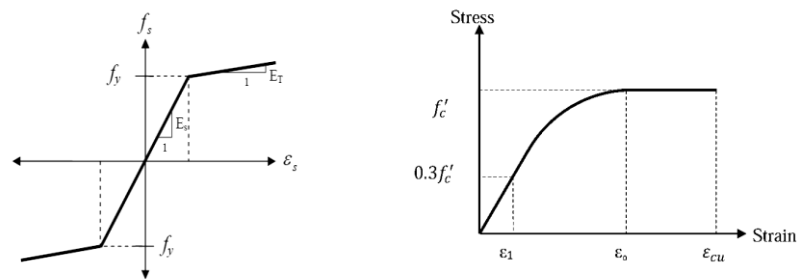


Figure 1. Experimental Specimen Details

A pair of headed studs with a diameter of $\phi 13\text{mm}$ and a length of 100mm was welded on the base steel plate having dimensions of 530mm \times 120mm \times 13mm. The average size of the stud head and the collar is shown with the test specimen. To increase the stiffness of the base plate and to provide sufficient resistance against plate bending, another steel plate known as a stiffener, having dimensions of 350mm \times 60mm \times 19mm was welded to the base plate on the other side. The concrete block had a concave section as shown in Figure 1, so that the specimen did not rotate during the application of load at the top of the base plate. The main objective of selecting the shape and size of the specimens was to realize easy application of various types of shear forces in the static and fatigue tests. Four 10mm diameter longitudinal deformed bars and two 6mm diameter stirrups of 200mm spacing as shown in Figure 1, were provided to overcome the premature cracks in the concrete block.

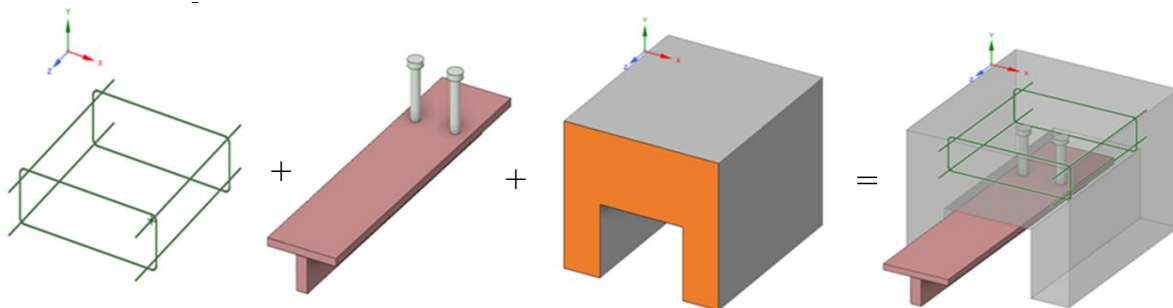
2.2 Material Properties of Structural Steel and Concrete

Structural steel was modeled using a bilinear isotropic hardening material model to represent its elastic–plastic behavior as shown in Figure 2(a). The initial portion of the stress–strain curve is linear, defined by the elastic modulus (E) and Poisson’s ratio (ν), up to the yield stress (f_y). Beyond yielding, plastic deformation occurs with strain hardening, represented by the tangent modulus. The concrete is assumed to be homogeneous and initially isotropic. In this study, a multilinear isotropic concrete material was adopted to evaluate the shear force–slip behavior of headed stud shear connectors. The compressive uniaxial stress–strain relationship for the concrete model was developed following the multi-linear isotropic stress–strain curve as shown in Figure 2(b). This material model was validated against experimental results.



(a) Steel (b) Concrete
Figure 2. Constitutive relations of steel and concrete materials

2.3 Numerical Modeling of the Experimental Specimen



(a) Rebar (b) Studs & baseplate (c) Concrete body (d) FE Model

Figure 3: Outline of the Finite Element Model

2.4 Boundary Conditions and FE Meshing

As shown in Figure 4(a), monotonic loading was applied as displacement at the top of the base plate (B), while the concrete block remained fixed at the top (C) and bottom (A). The load is applied as shown in Figure 4(b), where the abscissa is the number of loading steps and the ordinate represents the displacement in mm. In the analysis, 50 loading steps and a minimum of 30 sub-steps for each load step are used. Push and pull-out specimens were used to observe the numerical performance of headed stud shear connections under monotonic and cyclic loading. The cyclic displacement-controlled loading was selected based on the experimental procedures reported by Miah (2005) for pulsating and alternating shear forces on stud connectors. The amplitudes and number of cycles were chosen to ensure progressive nonlinear behavior of service-level cyclic actions in composite bridges. Bonded contact had been used at the baseplate and stud shear connector contact region. To facilitate numerical analysis, the concrete body and baseplate interface were made frictionless. The frictionless contact between the concrete block and baseplate was intentionally assumed to eliminate artificial and complex load transfer paths and ensure that the shear resistance is primarily governed by the stud shear connectors. The stud shear connector and the concrete body were in frictional contact. The friction coefficient of 0.35 represents a commonly adopted value for steel-concrete interfaces and has been widely used in numerical studies of composite structures (Li, 2024). The contact element was regarded as adjusted to touch for both frictional and frictionless contact. The mesh of the model is shown in Figure 4(c). Linear elements were used to create the finite element model. For the stud, base plate, and rebar, the multizone mesh technique was applied. For the base plate and stud shear connector, a 5mm element size was chosen. 15mm linear elements were used to mesh the concrete block. The contacts between the concrete and studs were refined with mesh. For improved numerical results, 2mm contact sizes were used at the stud and base plate contact regions. The selected mesh sizes were determined after several trial analyses, ensuring stable load–slip response and negligible change in peak shear capacity. The final mesh was chosen as an optimal balance between numerical accuracy and computational efficiency.

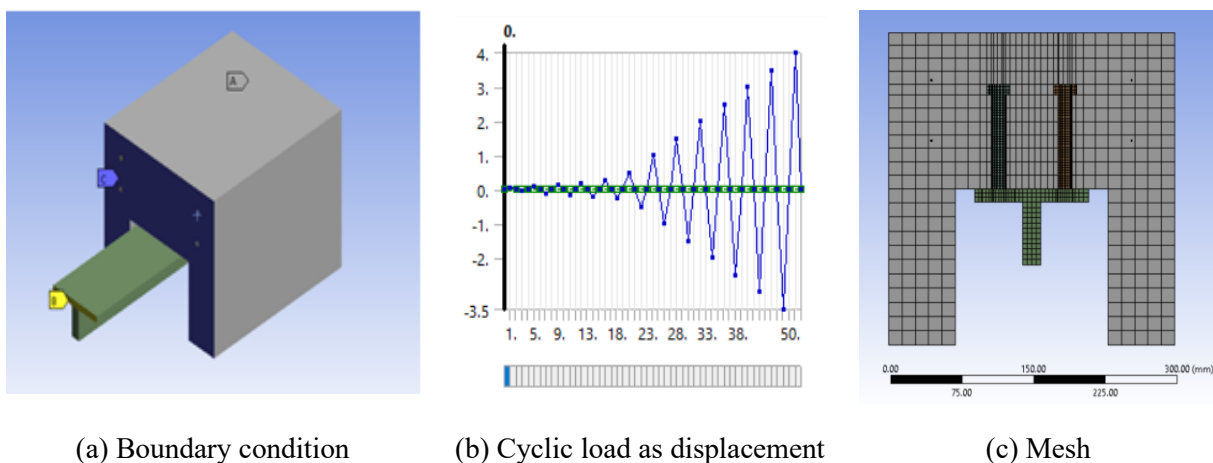


Figure 4: Boundary conditions and mesh and cyclic load of push and pull-out test specimen

2.5 Finite Element Modeling Parameters

The parameters that were used in the finite element (FE) study are listed in Table 1. The number M-C30D13 in this case M stands for monotonic loading, C for concrete strength, and D for the diameter of the stud shear connections. The word A in the name A-C30D13, on the other hand, stands for alternating load.

Table 1. Finite Element Model Parameters

	Stud Diameter (mm)	Stud Height (mm)	Strength of concrete (MPa)	Variable Parameters
Experimental	13	100	43.5	-
Analysis	13	100	43.5	-
M-C30D13	13	100	30	Stud Diameter (M)
M-C30D16	16	100	30	-
A-C30D13	13	100	30	Stud Diameter (A)
A-C30D16	16	100	30	-

To investigate the effect of stud diameter on the performance of the stud shear connectors, FE models were developed using an experimental reference specimen (Miah, 2005). The stud diameter and loading type were the parameters used in this study.

3. NUMERICAL RESULTS

The finite element models were analyzed under the prescribed loading and boundary conditions. This section presents the key findings on the behavior of stud shear connector under cyclic loading.

3.1 Validation of the FE Model

Test specimens geometry, material properties and boundary conditions were employed to validate the FE model. The shear force-slip relations obtained from the experiment (Miah, 2005) and FE simulations were observed and shown in Figure 4. From the experimental shear force-slip relation, the maximum shear force was found to be 58.9kN, whereas 61.85kN shear strength was found in the numerical analysis. The numerical shear strength varied by 3.4% from the experimental results. From Figure 4, it was found that the initial shear force-slip curve of the numerical analysis was very close to the experimental curve. But it was found that after the initial stage, the numerical curve differed slightly from the experimental curve. The variation was found due to the complexity in the geometry and contact behavior of the numerical model.

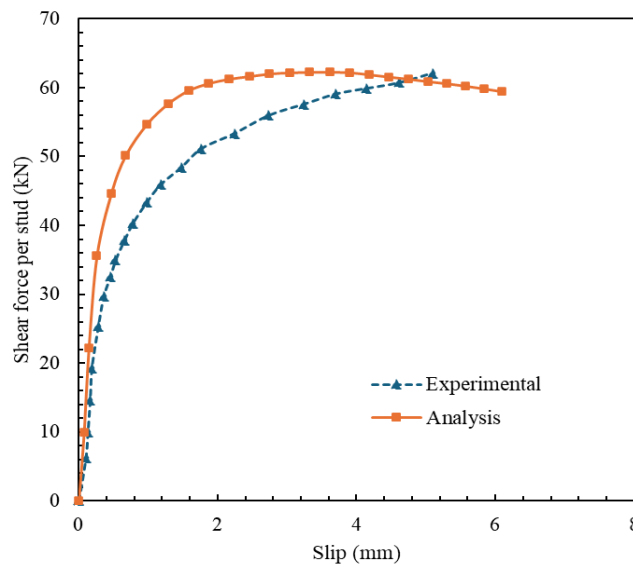


Figure 5. Shear force-slip relation for validation with experimental results

3.2 Shear Force and Slip Behavior for Monotonic and Cyclic Loads

The shear force–slip behavior of headed stud shear connectors with diameters of $\phi 13\text{mm}$ and $\phi 16\text{mm}$ under monotonic and cyclic loadings is shown in Figure 5, which is derived from finite element analysis in ANSYS Workbench. The vertical axis represents shear force per stud (kN), while the horizontal axis denotes slip (mm), allowing evaluation of the mechanical response under different loading regimes. Two distinct curves are plotted for each stud diameter, monotonic loading (M-C30D13 and M-C30D16) and cyclic loading (A-C30D13 and A-C30D16). The monotonic curves show a smooth, single-path progression, reflecting continuous shear resistance mobilization until peak capacity. In contrast, the cyclic curves exhibit hysteresis loops, characteristic of repeated loading and unloading, which highlight energy dissipation and stiffness degradation. For the $\phi 13\text{mm}$ stud (Figure 5a), the monotonic response demonstrates a gradual increase in shear force, reaching a lower peak compared to the $\phi 16\text{mm}$ stud. The cyclic response reveals wider hysteresis loops, indicating greater stiffness loss and more pronounced fatigue effects. This behavior suggests that smaller studs are more vulnerable to damage under cyclic loading, with reduced ability to sustain shear resistance over repeated cycles. The loops also show progressive slip accumulation, which is critical in assessing long-term performance in fatigue-prone environments.

In Figure 5b, the $\phi 16\text{mm}$ stud exhibits a higher peak shear force under monotonic loading, confirming the positive correlation between stud diameter and load-carrying capacity. The cyclic response also shows hysteresis loops, but they are narrower and more stable compared to the $\phi 13\text{mm}$ stud. This indicates improved cyclic durability and reduced stiffness degradation, making larger studs more suitable for applications involving repeated or dynamic loading. The enhanced performance can be attributed to the increased cross-sectional area and stronger mechanical interlock with surrounding concrete, which collectively improve shear resistance and fatigue behavior. The comparative analysis highlights that stud diameter significantly influences connector performance. Larger studs provide higher stiffness and strength under monotonic loading and exhibit superior energy dissipation with reduced degradation under cyclic conditions. These findings emphasize the importance of considering stud geometry in composite structure design, where shear connectors are critical for transferring loads between steel and concrete components. The presence of hysteresis loops under cyclic loading further underscores the necessity of accounting for fatigue effects in structures subjected to repetitive or dynamic forces.

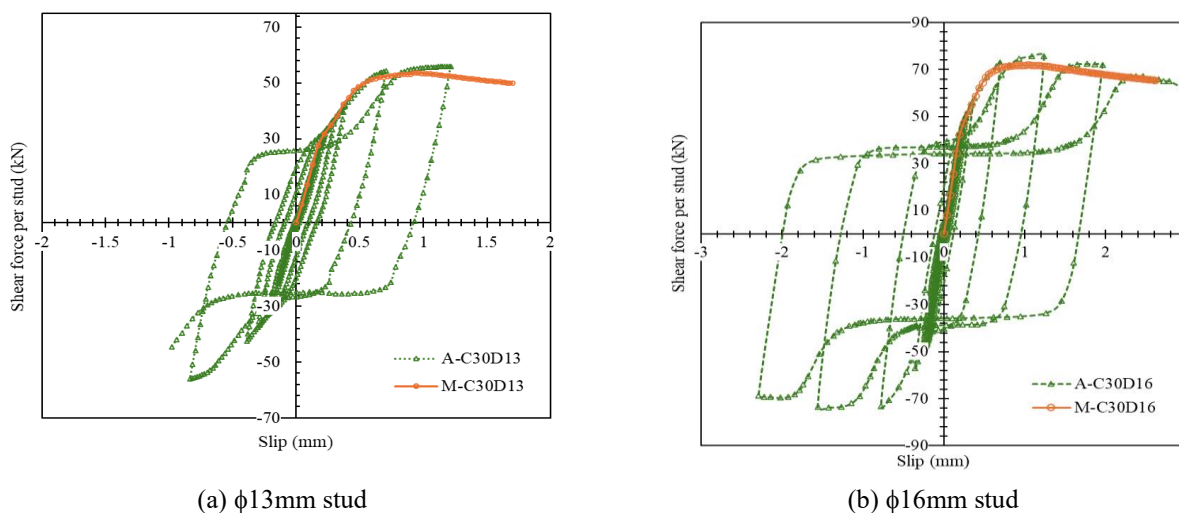


Figure 6. Shear force–slip relation under monotonic and alternating loads

3.3 Stiffness and Ductility

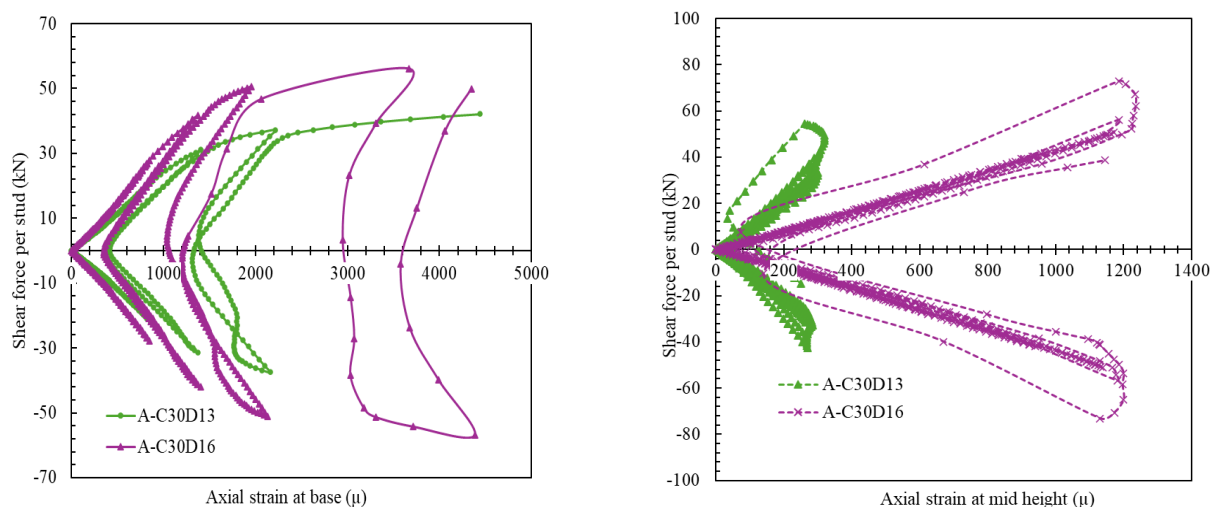
The initial shear stiffness of the stud shear connectors was evaluated from the linear portion of the monotonic load–slip curves, and the results indicate a clear influence of stud diameter on stiffness behavior. As per the previous research, the secant slopes corresponding to the interfacial slippage of 0.2mm were used as the shear stiffness values of studs in the elastic phases (Ye et al., 2022). The stiffness results under monotonic loads for both diameters ($\phi 13\text{mm}$ and $\phi 16\text{mm}$) is presented in Table 2, reflecting an increase of nearly 30% of stiffness for the $\phi 16\text{mm}$ stud. This higher stiffness in the connector is attributed to its larger cross-sectional area, which provides improved resistance to early-stage shear deformation and enhances the stud–concrete interaction. In contrast, the lower stiffness of the $\phi 13\text{mm}$ stud results in greater slip at comparable load levels, indicating a more flexible response. Under alternating loading, both studs experienced stiffness degradation, but the $\phi 16\text{mm}$ stud maintained superior stiffness retention and exhibited slower deterioration compared to the $\phi 13\text{mm}$ connector. The ultimate slip value was found to be 0.8mm and 1.0mm, respectively. The ductility behavior can be categorized based on the ultimate slip value of the stud (Zhao and Liu, 2018) as shown in the Table below.

Table 2. FEA results of the shear capacity of a single stud

Specimens	D (mm)	P_u (kN)	S_u (mm)	Stiffness(kN/mm)	Ductility
M-C30D13	$\phi 13\text{mm}$	55	0.8	75	Low
M-C30D16	$\phi 16\text{mm}$	75	1.0	100	Moderate

3.4 Shear Force and Axial Strain Relations

The shear force and axial strain relations for headed studs under alternating (cyclic) loading is shown in Figure 6. The axial strains are recorded at the base and mid-height for the $\phi 13\text{mm}$ (A-C30D13) and $\phi 16\text{mm}$ (A-C30D16) studs. At the base, both studs exhibit pronounced hysteresis loops, evidencing energy dissipation and cyclic stiffness degradation; the $\phi 13\text{mm}$ stud shows larger strain amplitudes and wider loops, indicating greater plasticity and damage concentration at the stud–concrete interface, whereas the $\phi 16\text{mm}$ stud maintains lower strain amplitudes and more stable loops, reflecting improved cyclic resilience.



(a) Axial strain at base (b) Axial strain at mid height of the stud
Figure 7. Shear force-strain relations for different diameters of stud under cyclic load

At mid-height, the loops are narrower for both diameters, demonstrating more elastic response and reduced strain localization compared to the base; again, the $\phi 13\text{mm}$ stud records higher cyclic strain

than the $\phi 16\text{mm}$ stud, consistent with its lower stiffness and capacity. Overall, the $\phi 16\text{mm}$ stud demonstrates superior cyclic performance at both measurement locations, with reduced strain demand and tighter hysteresis, while the $\phi 13\text{mm}$ stud exhibits higher localized deformation, especially at the base, highlighting diameter-dependent fatigue behavior and the importance of larger studs for enhanced durability under repeated loading.

3.5 Strain Behavior Along the Stud Shank

The variation of the axial strain along the height of the stud shank with two diameters ($\phi 13\text{mm}$ and $\phi 16\text{mm}$) embedded in C30 concrete is shown in Figure 7, for the shear forces ranging from 10kN to 40kN. In Figure 7, the ordinate indicates the axial strain and the abscissa indicates the height of the stud from the base to the head. The total height of the stud is 100mm, but the strain variation is shown for 92mm only, without the 8mm from the base. According to the graph, it is observed that the base of the stud shank is subjected to a large axial strain response. For all specimens, the axial strain is greatest at the stud base, where the welded connection to the steel beam serves as the primary shear-transfer interface, and decreases rapidly as the height increases. This demonstrates that the first 15mm length of the stud receives the majority of the load. The larger-diameter $\phi 16\text{mm}$ studs showed less strain than the $\phi 13\text{mm}$ studs under the same stress, indicating their superior stiffness and resistance to deformation caused greater strain along the entire stud length. Beyond mid-height, the strain profiles tend to stabilize for all load levels, with only minor variations near the stud head due to local confinement effects. The base strain plays an important role in the design of the stud shear connector as well as the prediction of the shear force transmission through the stud shank.

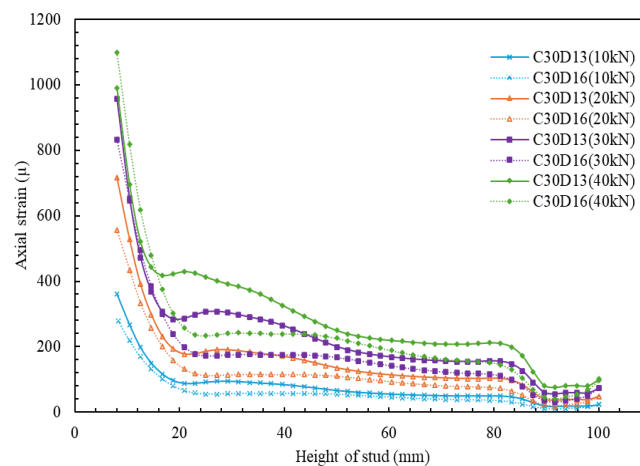


Figure 8. Strain behavior along the height of the stud shank

3.6 Vertical Distribution of Stud Deformation

The directional displacement variation along the height of the $\phi 16\text{mm}$ and $\phi 13\text{mm}$ stud shear connections under monotonic shear loads of 10kN, 20kN, 30kN, and 40kN is shown in Figure 8. The displacement is largest at the stud base for all loading levels and rapidly declines with height, reaching insignificant values close to the stud head. This pattern represents the expected concentration of shear deformation in the welded region, which is where the most load is transferred between the steel beam and concrete slab. The magnitude of displacement for both studs increases in proportion to the imposed monotonic load, demonstrating the gradual shift from elastic to nonlinear response. The $\phi 13\text{mm}$ stud shows greater deformation than the $\phi 16\text{mm}$ stud at all stress levels, demonstrating the larger-diameter connector's superior rigidity and load-carrying capacity. The smaller stud experiences significantly more slip at the base under the 40kN load, making the difference especially noticeable. Overall, the displacement profiles confirm the accuracy of the computational model in representing

the monotonic shear behavior of various stud diameters and match the distinctive fading pattern seen in stud shear connectors.

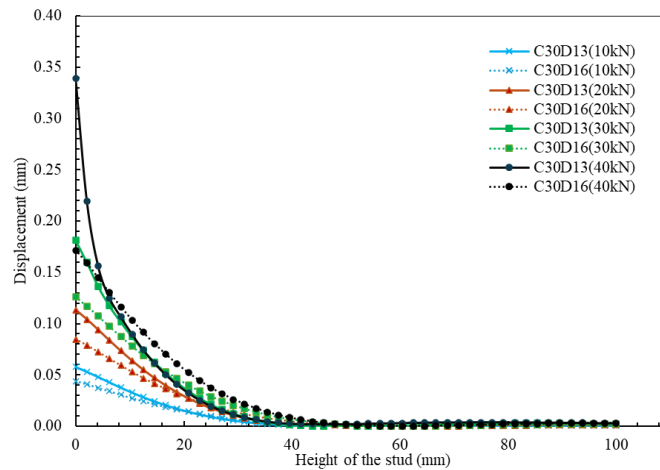
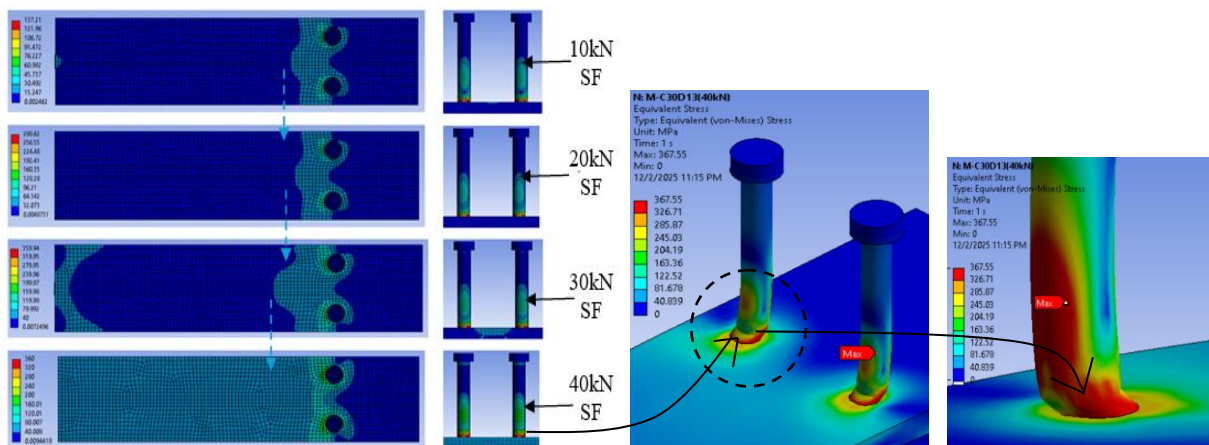


Figure 9. Vertical distribution of deformation along the height of the stud shank

3.7 Failure Modes

The von Mises stress distributions shown in Figure 9(a) for shear forces ranging from 10kN to 40kN clearly indicate the progressive development of stress concentration and the accompanying deformation mechanisms in the stud shear connector system. At low loading levels 10kN, stresses remain within the elastic range and are restricted predominantly to the stud base, where shear transfer initiates. The stress field spreads upward along the stud shank and outward into the surrounding concrete as the load reaches 20kN, indicating the beginning of nonlinear behavior and micro-cracking at the stud–concrete interface.



(a) Von Mises stress distribution

(b) Stress concentration and failure of stud

Figure 10. The distribution of Von Mises stress for different monotonic shear forces and failure of the stud at the base due to stress concentration

At 30kN, the stress concentration at the weld collar increased and stress begin entering deeper into the stud and concrete and onset of plastic deformation in the stud. The contact between stud and baseplate shows widespread stress propagation consistent with significant slide and degradation under the

maximum applied shear force of 40kN, whereas the stress contours show high-stress zones at the stud root as shown in Figure 9(b), confirming it as the major failure area. The stress patterns show that focused shear transfer causes failure to start at the stud base.

4. CONCLUSIONS

This study evaluated the performance of headed stud shear connectors under cyclic loading using ANSYS finite element numerical analysis. The numerical model was validated with experimental data, and the following conclusions can be summarized.

- (i) The $\phi 16\text{mm}$ stud exhibited higher shear strength and stiffness compared to the $\phi 13\text{mm}$ stud, confirming enhanced load-carrying capacity with increased stud diameter.
- (ii) Alternating loads caused hysteresis loops in both studs, with the $\phi 13\text{mm}$ stud showing wider loops and faster degradation, indicating greater fatigue sensitivity than the $\phi 16\text{mm}$ stud.
- (iii) Axial strain measurements revealed higher strain amplitudes at the base than mid-height, especially for the $\phi 13\text{mm}$ stud, leading to early plastic deformation and interface softening.
- (iv) Von Mises stress contours identified critical zones near the stud root and weld interface, with smaller studs showing earlier transition to failure.
- (v) The $\phi 16\text{mm}$ stud maintained more stable hysteresis loops, lower strain demand, and delayed yielding, making it more suitable for fatigue-prone composite structures.

ACKNOWLEDGEMENTS

The authors gratefully acknowledge the guidance and support received during this research. Appreciation is extended to the academic supervisors and collaborators whose constructive feedback and encouragement greatly contributed to the development of this study. The authors also acknowledge the technical assistance and facilities provided, which were essential for conducting the numerical analyses and completing the work successfully.

DECLARATION OF USE OF AI

The authors used artificial intelligence (AI) only to improve the language, grammar, clarity, and structure of the written content. The research concepts, methodology, data analysis, result interpretation, and technology findings were developed independently and without the use of AI technologies. The authors meticulously reviewed and confirmed every aspect of the work to ensure accuracy, originality, and compliance with academic and ethical standards.

REFERENCES

- Viest, I. (1956). "Investigation of stud shear connectors for composite concrete and steel T-beams." *ACI Journal Proceedings*, 52(4). doi:10.14359/11655.
- Feyissa, A. and Kenea, G. (2022). "Performance of shear connector in composite slab and steel beam with reentrant and open trough profiled steel sheeting." *Advances in Civil Engineering*. 2022, pp. 1–14. doi:10.1155/2022/5010501.
- Lu, K., Du, L., Xu, Q., Yao, Y. and Wang, J. (2023). "Fatigue performance of stud shear connectors in steel-concrete composite beam with initial damage." *Engineering Structures*. 276, p. 115381. doi:10.1016/j.engstruct.2022.115381.
- Wang, S., Feng, Z., Chen, G., Jiang, H. and Teng, S. (2021). "Numerical Analysis on shear behavior of grouped head stud shear connectors between steel girders and precast concrete slabs with high-strength concrete-filled shear pockets." *Journal of Bridge Engineering*. 26(6). doi:10.1061/(asce)be.1943-5592.0001727.
- Miah M. K. (2010). "Strain Behavior of Shear Connectors in Composite Structures." *DUET Journal*. Vol. 1, Issue 1, June 2010.
- Miah, M. K. (2005). "Behavior of stud shear connectors under pulsating and alternating shear forces." Ph. D Dissertation. Utsunomiya University, Japan.

- Ye, H.W., Huang, R., Tang, S.Q., Zhou, Y. and Liu, J.L. (2022). “*Determination of shear stiffness for headed-stud shear connectors using energy balance approach.*” *Steel Compos. Struct.* 42,477-487.
- Zhao, G. and Liu, Y. (2018). “*Finite element analysis of shear connector in composite beam under static load.*” *Engineering Structures.* 168, 879-892.
- Li, J.P., Zhang, L. Y., Zhu, Y. and Zhao, G. (2024) “*Finite element analysis of the flexural behavior of steel plate–high-performance concrete (HPC) slab and beam composite structures.*” *Buildings*, 15(1), p. 27. doi:10.3390/buildings15010027.